Superconductivity in the noncentrosymmetric compound Re_6Hf

Bin Chen,[1] Yang Guo,[1] Hangdong Wang,[1] Qiping Su,[1] Qianhui Mao,[2] Jianhua Du,[2] Yuxing Zhou,[2] Jinhu Yang,[1,*] and Minghu Fang[2,3,†]

[1]*Hangzhou Key Laboratory of Quantum Matter, Department of Physics, Hangzhou Normal University, Hangzhou 310036, China*

[2]*Department of Physics, Zhejiang University, Hangzhou 310027, China*

[3]*Collaborative Innovation Center of Advanced Microstructures, Nanjing 210093, China*

(Received 18 April 2016; published 22 July 2016)

Re_6Hf, which crystallizes in α-Mn structure(space group $I\bar{4}3m$) without a spatial inversion center, is a superconductor with a superconducting transition temperature $T_c \approx 6.2$ K. The measurements of magnetic susceptibility (χ), resistivity (ρ), and specific heat capacity (C) were carried out. Bulk superconductivity is revealed by the jump at T_c of the specific heat with $\Delta C/\gamma_n T_c \approx 1.63$, suggesting moderate electron-electron coupling strength in this system. The upper critical field $\mu_0 H_{c2}^{WHH}(0)$ was estimated to be of 89 kOe, and $\mu_0 H_{c2}^{GL}(0) = 107$ kOe, which is close to the Pauli limiting field. The Ginzburg Landau parameter $\kappa_{GL} = 50.2$, indicates that Re_6Hf is a type-II superconductor. The temperature dependence of the electronic specific heat $C_{el}(T)$ in the superconducting state can be explained by BCS theory. Furthermore, the magnetic-field dependence of $\gamma(H)$ is found to be linear with respect to H. These results imply a dominant s-wave superconductivity in Re_6Hf.

DOI: 10.1103/PhysRevB.94.024518

I. INTRODUCTION

The superconductivity discovered in a heavy fermion compound $CePt_3Si$ without an inversion symmetry, has stimulated considerable interest in theoretical and experimental research in recent years [1]. Theoretically the parity conservation may be broken with increasing the strength of asymmetric spin-orbit coupling (ASOC) in materials with noncentrosymmetric structure. Therefore the superconducting state may exhibit an admixture of spin-singlet and spin-triplet components. To date, a number of noncentrosymmetric superconducting compounds have been investigated. For example, $CePt_3Si$ [1], $CeRhSi_3$ [2], $CeIrSi_3$ [3], $CeCoGe_3$ [4], and $CeIrGe_3$ [5] are antiferromagnets at ambient pressure while exhibiting superconductivity under high pressure. However, the complexity of the f-electron magnetism may mask the nature of noncentrosymmetric superconductivity. It is, therefore, important to search for f-electron free compounds lacking inversion symmetry in order to study noncentrosymmetric superconductivity. For some d-electron systems, a dominant characteristic of conventional Bardeen-Cooper-Schrieffer (BCS) superconductivity has been reported in Ru_7B_3 [6], $Mg_{12-\delta}Ir_{19}B_{16}$ [7], Li_2Pd_3B [8], and Re_3W [9]. The absence of a Hebel-Slichter peak in the spin-lattice relaxation rate and a power law temperature dependence of the specific heat in Mo_3Al_2C indicate unconventional superconductivity in this system [10]. Muon spin relaxation (μSR) experiments suggests that the time-reversal symmetry is broken in the superconducting state in $LaNiC_2$ and four triplet states are possible in this system [11]. Furthermore, superconductivity in some rhenium alloys $Re_{24}T_5$ (T = Ti and Nb) were reported previously, which crystallize in the noncentrosymmetric structure of a cubic α-Mn type with the space group $I\bar{4}3m$ (No. 217). For example, $Re_{24}Ti_5$ [12] is a superconductor with a T_c of 5.8 K. $Nb_{0.18}Re_{0.82}$ is a moderately coupled superconductor and the upper critical field is comparable with the calculated Pauli limit. Point contact spectroscopy results provide evidence of two-gap superconductivity [13]. ^{93}Nb NMR results show a coherence peak below T_c, indicating a conventional superconductivity in $Re_{24}Nb_5$ [14,15].

Recently, transverse-field μSR experiments show s-wave character for the superconducting gap in Re_6Zr [16] which adopts the same structure as $Re_{24}Ti_5$, however, zero- and longitudinal-field μSR data reveal spontaneous static magnetic fields below T_c which means a broken time-reversal symmetry in the superconducting state and an unconventional pairing mechanism. The isostructural compound $Re_{0.86}Hf_{0.14}$ (this can also be written as $Re_6Hf_{0.98}$) is a superconductor with a T_c of 5.86 K as reported by Matthias *et al.* in 1963 [17]. Since Hf atoms are heavier than Ti, Zr, or Nb atoms, the ASOC strength is expected to be enhanced which can lead to the admixture of spin-singlet and spin-triplet order as discovered in $Li_2(Pt, Pd)_3B$ [8,18,19].

Here we report on the synthesis and characterization of polycrystalline Re_6Hf which showed a bulk superconducting transition at $T_c \approx 6.2$ K. We measured the powder x-ray diffraction to determine its crystal structure. The superconducting properties for Re_6Hf were studied by the measurements of magnetic susceptibility, electrical resistivity, and specific heat capacity. The superconducting parameters of Re_6Hf, such as the thermodynamic critical field H_{c0} and the lower and upper critical field H_{c1} and H_{c2}, the coherence length $\xi(0)$, the electronic specific heat coefficient γ_n, and the specific heat jump $\Delta C/\gamma_n T_c$ were estimated. The electronic heat capacity decreases exponentially with decreasing temperature and the magnetic dependence of $\gamma(H)$ shows linear behavior. Our results suggest that the superconductivity in Re_6Hf is of s-wave gap symmetry.

II. EXPERIMENTAl DETAILS

A polycrystalline sample was prepared by melting stoichiometric amounts of high-purity Re (99.9%), and Hf (99.9%) in an arc furnace, filled with pure argon gas (99.99%), using

*yjhphy@hznu.edu.cn
†mhfang@zju.edu.cn

a tungsten electrode and a water-cooled copper hearth. A Ti button was used as an oxygen getter. The samples were melted several times in order to improve homogeneity and formed a hemispherical ingot with negligible mass loss. Then, the ingot was annealed in a vacuum-sealed quartz tube at 1123 K for 1 week, followed by cooling to room temperature in 24 hours. The obtained sample is brittle and easily ground into powder for powder x-ray diffraction measurement. A room-temperature powder x-ray diffraction pattern was taken with Cu $K\alpha$ radiation on the powdered sample. A small rectangular bar was cut using a diamond saw for the resistivity and specific heat capacity measurements. The electrical resistivity was measured using a standard four-probe method in a dc magnetic field up to 90 kOe and the lowest temperature is 2 K. The magnetic susceptibility and specific heat measurements were performed in a commercial magnetic property measurement system (7 T) and a physical property measurement system (9 T), respectively.

III. RESULTS AND DISCUSSION

Figure 1 shows the x-ray diffraction pattern measured at room temperature. The diffractometer pattern shows no impurity phase. The lattice constant of the prepared sample was determined to be 9.678 ± 0.002 Å by using the Rietveld method with a general structure analysis system [20]. The refinements gave Hf(1) site ($2a$ in Wyckoff notation) (0,0,0), Hf(2) site ($8c$) (0.3106,0.3106,0.3106), Re(1) site ($24g$) (0.3623,0.3623,0.0383), and Re(2) site ($24g$) (0.6954,0.6954,0.2903). Hf(1) site has an inversion center, while the Hf(2), Re(1), and Re(2) sites have no inversion center in the structure.

Figure 2 displays the temperature dependence of magnetic susceptibility(χ) measured at an applied field of 10 Oe. Superconductivity defined as the onset of the diamagnetic

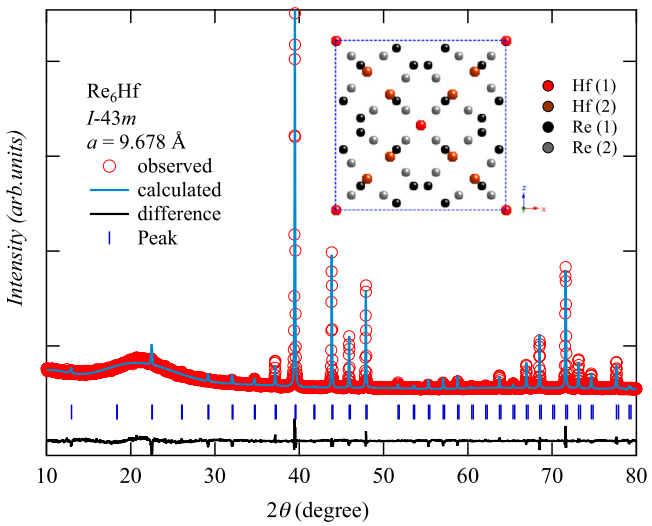

FIG. 1. Rietveld refinement for the Re_6Hf sample. The red circles correspond to the experimental data. The blue solid line shows the calculated pattern. The blue vertical bars give the Bragg positions for the phase Re_6Hf of space group $I\bar{4}3m$. The black line at the bottom of the plot displays the difference between the experimental and calculated patterns.

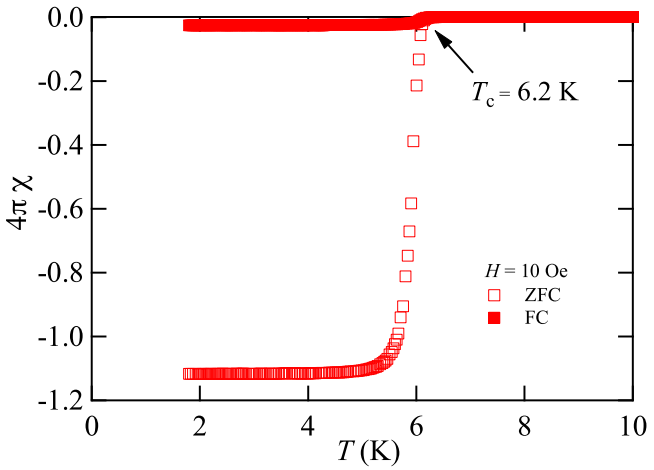

FIG. 2. Zero-field-cooled (ZFC) and field-cooled (FC) magnetic susceptibility of Re_6Hf at an applied magnetic field of 10 Oe.

signal in the magnetization as indicated by an arrow as shown in Fig. 2, occurs at $T_c = 6.2 \pm 0.1$ K. The value of $4\pi\chi$ (2 K) exceeds -1 due to the demagnetization effect. The susceptibility measured at an applied magnetic field of 1 kOe, remains almost constant at 8.8×10^{-4} cm^3/mol from 7 to 300 K. Generally, the susceptibility $\chi = \chi_{\text{core}} + \chi_{vv} + \chi_L + \chi_P$, where χ_{core} is the diamagnetic core susceptibility, χ_{vv} the paramagnetic Van Vleck susceptibility, χ_L the Landau diamagnetic susceptibility of the conduction carriers, and the last term, χ_P, the Pauli spin susceptibility of the conduction carriers. We estimated $\chi_{\text{core}} = -4.32 \times 10^{-4}$ cm^3/mol using Hartree-Fock approximations [21]. The χ_P is evaluated from the relation $\chi_P = (g^2/4)\mu_B^2$, where g is the spectroscopic splitting factor of the conduction carriers, μ_B the Bohr magneton, and $D(E_F)$ the band-structure density of states at the Fermi energy E_F. Using $g = 2$ and $D(E_F) =$ 6.4 states/eV f.u. (estimated from specific heat as explained below), $\chi_P = 2.08 \times 10^{-4}$ cm^3/mol. Assuming the band-structure effective mass $m^* = m_e$, where m_e is the mass of free electron, we obtained $\chi_L = -6.9 \times 10^{-5}$ cm^3/mol from the formula $\chi_L = -1/3(m^*/m_e)\chi_P$. Therefore, χ_{vv} is derived as 11.4×10^{-4} cm^3/mol.

The temperature dependence of the electrical resistivity of Re_6Hf between 2 and 300 K is shown in Fig. 3(a). The resistivity decreases with decreasing temperature, indicating a metallic behavior. A superconducting transition with an onset temperature $T_c^{\text{onset}} = 6.4$ K (the temperature at which the resistivity has decreased by 10% from its normal state value just above T_c) and the resistivity goes to zero at $T_c =$ 6.2 K which coincides with the result of the superconducting transition temperature determined from the susceptibility. The superconducting transition temperature width is about 0.2 K, indicating the high quality of our sample. The resistivity has little dependence on temperature and the residual resistivity ratio($\rho_{300\text{ K}}/\rho_{7\text{ K}}$) is only 1.08. The small residual resistivity ratio was also observed in other compounds with the same structure [12,14]. This means the resistivity of the polycrystalline sample with $I\bar{4}3m$ space group is sensitive to impurities or/and disorder.

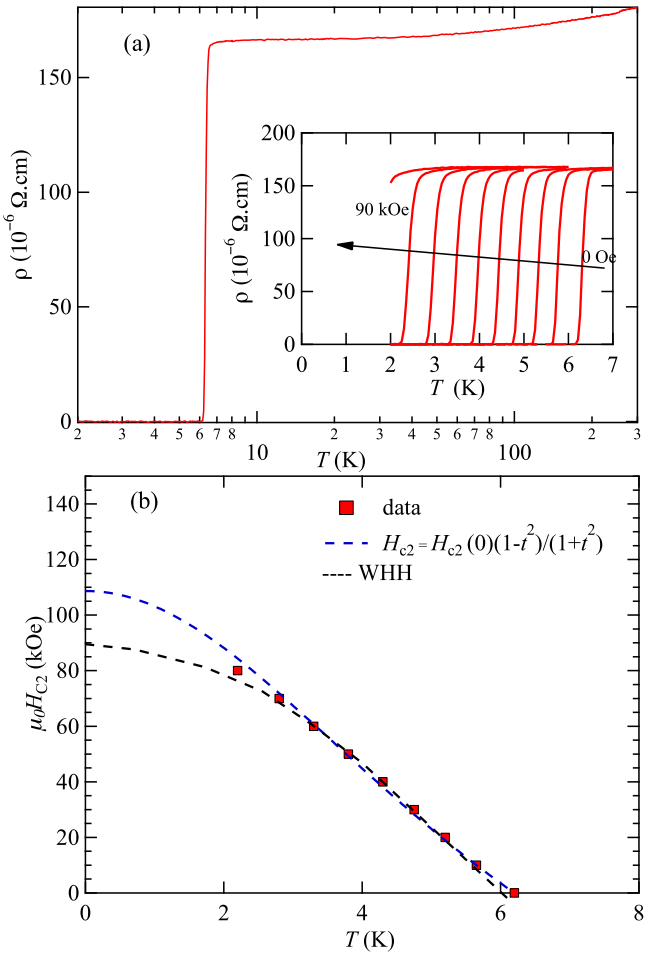

FIG. 3. (a) Temperature dependence of the electrical resistivity of Re_6Hf between 2 and 300 K, and (b) upper critical field of Re_6Hf as a function of temperature. The H_{c2} data is derived from a 90% drop in resistivity from its normal state value just above T_c. The upper inset shows the superconducting transition temperature is depressed under magnetic fields up to 90 kOe gradually.

Now we present the analysis of the upper critical field of H_{c2}, obtained from a 90% drop of the normal-state resistivity just above T_c. $H_{c2}(T)$ shows an almost linear temperature dependence as displayed in Fig. 3(b) and the initial slope near T_c is estimated as $-(20.9 \pm 0.2)$ kOe/K. For a dirty type-II superconductor, the Werthamer-Helfand-Hohenberg (WHH) [22] gives $\mu_0 H_{c2}^{WHH}(0) = (89 \pm 4)$ kOe from the relation

$$\mu_0 H_{c2}^{WHH}(0) = 0.693 \left(\frac{d\mu_0 H_{c2}}{dT} \right)_{T_c} T_c. \qquad (1)$$

We also evaluated the upper critical field from Ginzburg-Landau formula $\mu_0 H_{c2}(T) = \mu_0 H_{c2}(0)(1-t^2)/(1+t^2)$, where t is the normalized temperature T/T_c. The fitting curve, shown as a blue dashed line in Fig. 3(b), agrees with the data quite well. The upper critical field $\mu_0 H_{c2}^{GL}(0) = (107 \pm 1)$ kOe, which is close to the Pauli limiting field (113 ± 4) kOe, derived from the relation $\mu_0 H_P = 1.83 \times 10^4 T_c$. In fact, Eq. (1) corresponds to $\alpha = 0$ and $\lambda_{so} = 0$, where α is the Maki parameter and λ_{so} the spin-orbit pair breaking

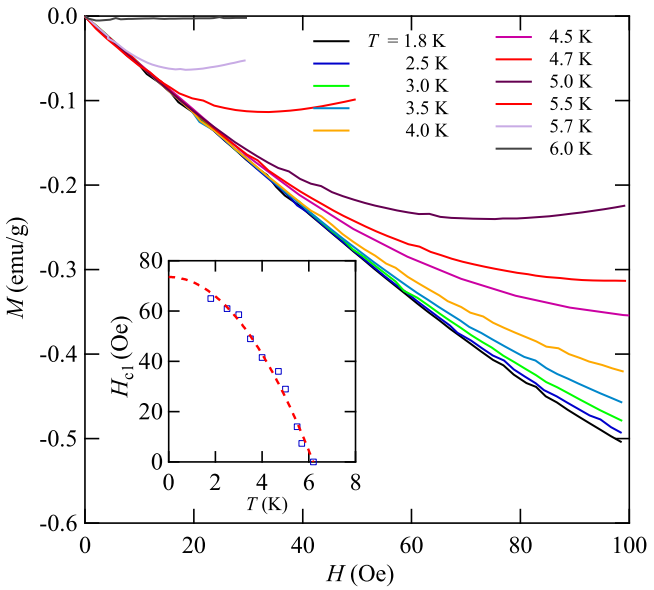

FIG. 4. Magnetization with an applied magnetic field at different temperatures. Inset: lower critical field H_{c1} determined at the magnetic field where the deviation of the magnetization from its linear relation with the applied field occurs.

parameter. Experimentally, the Maki parameter can be derived from the relation $\alpha = 0.53(-dH_{c2}/dT)_{T_c}$ [23]. Therefore α is estimated as 1.11 ± 0.05, which is also consistent with the result from the relation $\alpha = \sqrt{2} H_{c2}^{WHH}/H_P$. The Maki parameter can be expressed as $\alpha = \frac{3e^2\hbar\gamma\rho_0}{2m\pi^2 k_B^2}$, where e is the electron charge and m the electron mass [22]. Taking the α estimated above and the Sommerfeld value γ_n (see below) yields the intrinsic intragranular resistivity $\rho \approx 80 \pm 4\ \mu\Omega$ cm.

In order to obtain the superconducting parameters, we estimated the lower critical field $\mu_0 H_{c1}$ from $M(H)$ in low magnetic fields. The sample used for the measurement was about $2.8 \times 0.8 \times 0.8$ mm^3. The demagnetization factor for the sample is derived from $N_m = \frac{2}{\pi} \arcsin \frac{1}{1+2r} \approx 0.14$, where $r = c/a$ (c,a is the length and the width of the sample, respectively). The actual magnetic field in the sample was corrected by taking demagnetization effect into account. The lower critical field H_{c1} defined as the magnetization deviation from its linear relation with magnetic field in the M-H plot is shown in Fig. 4. We fit the data according to the formula $H_{c1} = H_{c1}(0)(1-(T/T_c)^2)$, which yields $\mu_0 H_{c1}(0) = 74 \pm 2$ Oe. With these results for $H_{c1}(0)$ and $H_{c2}(0)$, we can estimate several superconducting parameters for Re_6Hf. From $\xi_{GL}^2 = \Phi_0/2\pi\mu_0 H_{c2}$, where Φ_0 is the quantum flux ($h/2e$), we find a Ginzburg-Landau coherence length $\xi_{GL}(0) = 61.2 \pm 0.3$ Å. A penetration depth, $\lambda_{GL}(0) = (3.06 \pm 0.04) \times 10^3$ Å is obtained from $\mu_0 H_{c1} = \Phi_0/4\pi\lambda_{GL}^2(0) \ln[\lambda_{GL}(0)/\xi_{GL}(0)]$. The Ginzburg-Landau parameter $\kappa(0) = \lambda_{GL}(0)/\xi_{GL}(0) = 50.2 \pm 0.9$. Using these parameters and the relation $H_{c1} H_{c2} = H_c^2 \ln\kappa$, we find that the thermodynamic critical field $\mu_0 H_c(0) = (1.26 \pm 0.03)$ kOe.

The plot of C_p/T versus T^2 at $H = 0$ is shown in Fig. 5. The specific heat capacity data in the normal state allows the determination of the Sommerfeld constant (γ) and

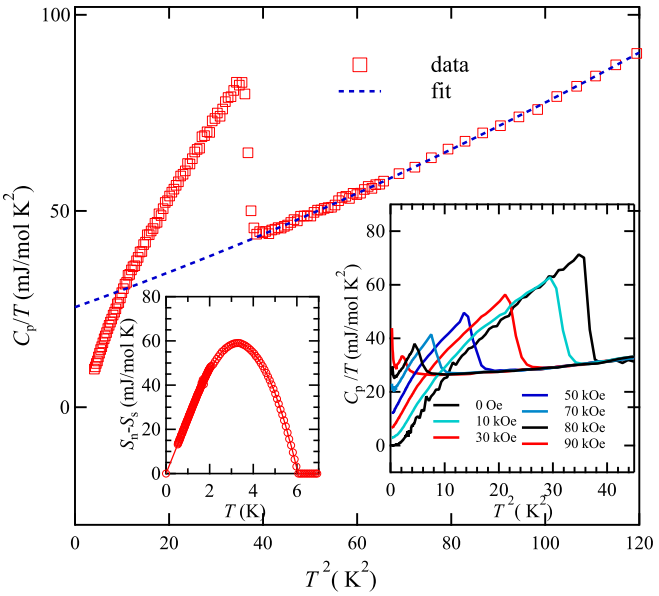

FIG. 5. Temperature dependence of the specific heat capacity of Re_6Hf plotted as C_p/T vs T, which shows bulk superconductivity at $T_c \approx 6.2$ K. The dashed line is the best fit to the data by the Debye model at low temperatures. The left inset shows the conservation of entropy and the C_p/T vs T^2 under various magnetic fields is shown in the right inset. An upturn appears in the curve under the magnetic field larger than 70 kOe at lower temperatures, which is probably due to a Schottky anomaly.

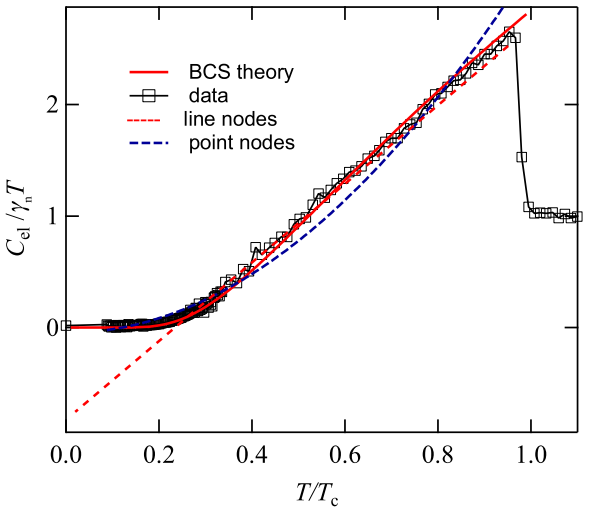

FIG. 6. The reduced temperature dependence of the electronic specific heat $C_{el}/\gamma_n T$ of Re_6Hf in the superconducting state. The solid and dashed lines are fits to the data as described in the text.

Debye constant (β) from $C_p(T) = \gamma T + \beta T^3 + \delta T^5$. The dotted line represents the best fit to the data which yields $\gamma = 25.3 \pm 0.6$ mJ/mol K^2, $\beta = 0.43 \pm 0.02$ mJ/mol K^4, and $\delta = 0.9 \pm 0.1$ μJ/mol K^6. The Debye temperature Θ_D, evaluated from the relation $\Theta_D = (12\pi^4 RN/5\beta)^{1/3}$, where $R = 8.31$ J/mol K and N is the number of atoms in unit cell of Re_6Hf, is 316 ± 5 K. With Θ_D and T_c, we calculated the electron-phonon constant $\lambda_{ep} = 0.67 \pm 0.01$ by means of the McMillan equation [24]

$$\lambda_{ep} = \frac{1.04 + \mu^* \ln\left(\frac{\theta_D}{1.45T_c}\right)}{(1 - 0.62\mu^*)\ln\left(\frac{\theta_D}{1.45T_c}\right) - 1.04}, \qquad (2)$$

where μ^* is the Coulomb pseudopotential of about 0.13 used in intermetallic superconductors. This value is comparable to those in noncentrosymmetric superconductors, such as 0.68 for $Mg_{10}Ir_{19}B_{16}$ [7] and 0.5 for $LaRhSi_3$ [25], indicating that the electron-phonon coupling is moderately strong in Re_6Hf. Generally, γ_n relates the electronic density of states around the Fermi level. The Fermi level density of states $D(E_F)$ estimated using the values of γ and λ_{ep} according to the relation $\gamma_n = \frac{\pi^2 k_B^2}{3} D(E_F)[1 + \lambda_{ep}]$. Therefore $D(E_F)$ is estimated as 6.4 ± 0.2 states/eV f.u. The specific-heat jump $(\Delta C/T_c)$ for Re_6Hf is about 41.3 ± 0.7 mJ/mol K^2, which gives a value of $\Delta C/\gamma_n T_c = 1.63 \pm 0.05$, slightly larger than 1.43 predicted by BCS theory. The condensation energy, $U(0)$, was estimated from

$$\Delta U(0) = -\frac{\gamma_n T_c^2}{2} + \int_0^{T_c} C_{el}(T) dT, \qquad (3)$$

subjected to the entropy-conserving fit for the specific heat. Using $\gamma_n = 25.3$ mJ/mol K^2 and $T_c = 6.2$ K, we obtained $\Delta U(0) = 245 \pm 10$ mJ/mol. The thermodynamic critical is estimated to be 936 ± 20 Oe using the relationship $\Delta U(0) = 1/2\mu_0 H_c^2(0)$, which is consistent with the value determined by the critical fields.

The electronic specific heat at very low temperatures gives key information about the superconducting gap structure. Therefore we obtained C_{el} by subtracting the lattice contribution from the total heat capacity. The reduced temperature dependence of the electronic specific heat $C_{el}/\gamma_n T$ below T_c is shown in Fig. 6. Within the framework of BCS theory, the superconducting contribution to the entropy (S) is calculated as

$$S = -\frac{6\gamma_n \Delta_0}{\pi^2 k_B} \int_0^\infty [f \ln f + (1 - f)\ln(1 - f)] dy, \qquad (4)$$

where $f = \frac{1}{1+e^{\beta E}}$ and $\beta = \frac{1}{k_B T}$. The energy of the quasiparticles is $E = \Delta_0 \sqrt{y^2 + \Delta(T)^2}$, where Δ_0 is the superconducting gap and $y = \epsilon/\Delta_0$ is the electron energy at the normal state. $\Delta(T)$ is the temperature dependence of the BCS superconducting gap as calculated by Mühlschlegel [26]. The electronic specific heat is thereafter calculated by $C_{el} = TdS/dT$. We set γ_n and Δ_0 as adjustable parameters. The fit agrees with the data in the whole temperature range below T_c and the results yield $\gamma_n = 24.1 \pm 0.3$ mJ/mol K and $\Delta_0 = 1.02 \pm 0.03$ meV. The ratio $\Delta_0/k_B T_c = 1.91 \pm 0.03$ is larger than the value 1.76 as predicted for a weak coupling limit, suggesting that the electron-electron is moderately coupled in Re_6Hf. In order to check other gap symmetry in Re_6Hf, we fit the data according to the formulas $C_{el}/\gamma_n T \propto T, T^2$ as expected for line nodes and point nodes, respectively. The fit coincides with the data in the temperature of $0.25 \leqslant T/T_c \leqslant 1$ for the gap with line nodes, however, a strong deviation occurs below $T/T_c \approx 0.25$. The fit agrees with the data below $T/T_c \approx 0.38$ for the gap with point nodes and departs from the data in the range of $0.38 \leqslant T/T_c \leqslant 1$. Overall, these two models cannot describe

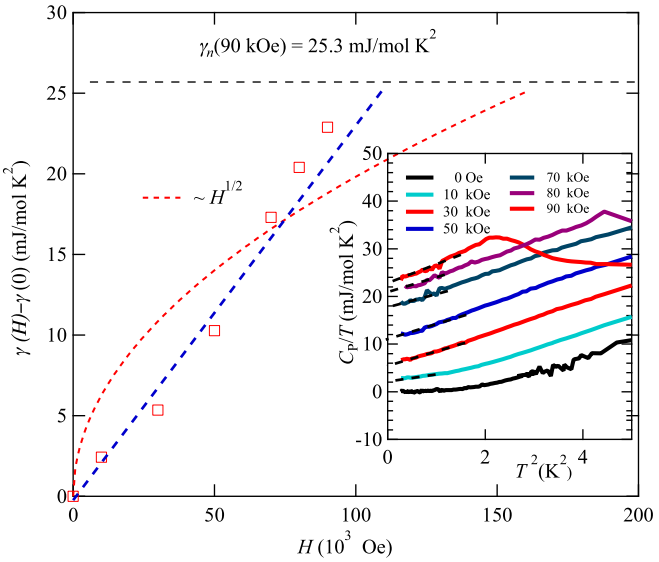

FIG. 7. Sommerfeld parameter γ_H as a function of magnetic field. The solid line indicates a linear dependence as predicted for an s-wave gap structure, the dotted line represents the dependence expected for an anisotropic gap or a gap with nodes. γ_H is estimated by extrapolating the data to zero temperature in C_p/T vs T^2 plots.

the temperature dependence of the electronic specific heat in the superconducting state in Re_6Hf.

A clear upturn appears in the curve above 70 kOe at very low temperatures as shown in the right inset of Fig. 5, which is probably due to a nuclear Schottky anomaly. The Schottky anomaly was also discovered by Yuan *et al.* in $Nb_{0.18}Re_{0.82}$ [27]. We noticed that the nuclear-quadrupole interaction in rhenium metal can produce an upturn in specific heat at low temperatures [28]. Therefore the Schottky anomaly in Re_6Hf may come from a small amount of unreacted Re, which cannot be detected by x-ray diffraction. In order to get more information on the Cooper pairing in Re_6Hf, we remove the Schottky anomaly by fitting the data in the temperature region between 0.5 and 2 K according to the equation $C_{\text{Schottky}} \propto \frac{A}{T^2}\exp(-\varepsilon/KT) + B/T^2$ [29]. Thus we obtained the Sommerfeld constant $\gamma(H)$ under different magnetic field as shown in Fig. 7. In theory, a nonlinear behavior $\gamma(H) \propto H^{1/2}$ is predicted for a highly anisotropic gap or a gap with nodes, and $\gamma(H)$ is proportional to the number of field-induced vortices, i.e., $\gamma(H) \propto H$ for a fully gapped superconductivity. It can be seen that $\gamma(H)$ shows strong deviation from $H^{1/2}$ behavior and good linear dependence with the applied magnetic field. That the field linear increases in $\gamma(H)$ provides further evidence of a dominant s-wave superconductivity in Re_6Hf. However, the linear temperature dependence of the upper critical field $H_{c2}(T)$ and $H_{c2}(0)$ close to the Pauli limiting field behavior are unusual for a simple BCS-type superconductor. Other pairing symmetries cannot be ruled out since the impurity and/or disorder in our polycrystalline sample may mask the intrinsic behavior at low temperatures in Re_6Hf.

IV. SUMMARY

Polycrystalline samples of Re_6Hf were prepared by arc melting. The result of x-ray diffraction measurement confirms a pure phase with the noncentrosymmetric α-Mn-type structure. We investigated the physical properties of the noncentrosymmetric superconductor Re_6Hf by measuring magnetic susceptibility, electrical resistivity, and specific heat capacity. Our main results show that Re_6Hf displays a type-II superconductivity at $T_c = 6.2$ K. The value of $\Delta C/\gamma_n T_c = 1.63$ indicates the compound is in moderate coupling regime. The electronic specific heat C_{es} shows an exponential behavior at low temperatures, and $\gamma(H) \propto H$, suggesting a dominant s-wave pairing in Re_6Hf, However there is still the possibility of an admixture of spin-singlet and spin-triplet pairing states since the disorder effect may mask the gap anisotropy. Research on high quality of single crystals of Re_6Hf is needed in the future to clarify the nature of the superconducting pairing in this system.

ACKNOWLEDGMENTS

This research is supported by the National Basic Research Program of China (973 Program) under Grants No. 2016YFA0300402, No. 2015CB921004, and No. 2012CB821404, the Nature Science Foundation of China (Grants No. 11374261 and No. 11204059) and Zhejiang Provincial Natural Science Foundation of China (Grant No. LY14A040007), and the Fundamental Research Funds for the Central Universities of China.

[1] E. Bauer, G. Hilscher, H. Michor, Ch. Paul, E. W. Scheidt, A. Gribanov, Yu. Seropegin, H. Noël, M. Sigrist, and P. Rogl, Phys. Rev. Lett. **92**, 027003 (2004).

[2] N. Kimura, K. Ito, K. Saitoh, Y. Umeda, H. Aoki, and T. Terashima, Phys. Rev. Lett. **95**, 247004 (2005).

[3] I. Sugitani, Y. Okuda, H. Shishido, T. Yamada, A. Thamizhavel, E. Yamamoto, T. D. Matsuda, Y. Haga, T. Takeuchi, R. Settai, and Y. Ōnuki, J. Phys. Soc. Jpn. **75**, 043703 (2006).

[4] R. Settai, I. Sugitani, Y. Okuda, A. Thamizhavel, M. Nakashima, Y. Onuki, and H. Harima, J. Magn. Magn. Mater. **310**, 844 (2007).

[5] F. Honda, I. Bonalde, K. Shimizu, S. Yoshiuchi, Y. Hirose, T. Nakamura, R. Settai, and Y. Ōnuki, Phys. Rev. B **81**, 140507 (2010).

[6] L. Fang, H. Yang, X. Zhu, G. Mu, Z.-S. Wang, L. Shan, C. Ren, and H.-H. Wen, Phys. Rev. B **79**, 144509 (2009).

[7] G. Mu, Y. Wang, L. Shan, and H.-H. Wen, Phys. Rev. B **76**, 064527 (2007).

[8] K. Togano, P. Badica, Y. Nakamori, S. Orimo, H. Takeya, and K. Hirata, Phys. Rev. Lett. **93**, 247004 (2004).

[9] Y. L. Zuev, V. A. Kuznetsova, R. Prozorov, M. D. Vannette, M. V. Lobanov, D. K. Christen, and J. R. Thompson, Phys. Rev. B **76**, 132508 (2007).

[10] E. Bauer, G. Rogl, X.-Q. Chen, R. T. Khan, H. Michor, G. Hilscher, E. Royanian, K. Kumagai, D. Z. Li, Y. Y. Li, R. Podloucky, and P. Rogl, Phys. Rev. B **82**, 064511 (2010).

[11] A. D. Hillier, J. Quintanilla, and R. Cywinski, Phys. Rev. Lett. **102**, 117007 (2009).
[12] C. S. Lue, H. F. Liu, C. N. Kuo, P. S. Shin, J.-Y. Lin, Y. K. Kuo, M. W. Chu, T.-L. Hung, and Y. Y. Chen, Supercond. Sci. Technol. **26**, 055011 (2013).
[13] C. Cirillo, R. Fittipaldi, M. Smidman, G. Carapella, C. Attanasio, A. Vecchione, R. P. Singh, M. R. Lees, G. Balakrishnan, and M. Cuoco, Phys. Rev. B **91**, 134508 (2015).
[14] A. B. Karki, Y. M. Xiong, N. Haldolaarachchige, S. Stadler, I. Vekhter, P. W. Adams, W. A. Phelan, and J. Y. Chan, Phys. Rev. B **83**, 144525 (2011).
[15] C. S. Lue, T. H. Su, H. F. Liu, and B.-L. Young, Phys. Rev. B **84**, 052509 (2011).
[16] R. P. Singh, A. D. Hillier, B. Mazidian, J. Quintanilla, J. F. Annett, D. McK. Paul, G. Balakrishnan, and M. R. Lees, Phys. Rev. Lett. **112**, 107002 (2014).
[17] B. T. Matthias, T. H. Gebave, and V. B. Compton, Rev. Mod. Phys. **35**, 1 (1963).
[18] H. Q. Yuan, D. F. Agterberg, N. Hayashi, P. Badica, D. Vandervelde, K. Togano, M. Sigrist, and M. B. Salamon, Phys. Rev. Lett. **97**, 017006 (2006).
[19] P. Badica, T. Kondo, and K. Togano, J. Phys. Soc. Jpn. **74**, 1014 (2005).
[20] A. C. Larson and R. B. Von Dreele, General structure analysis system (GSAS), Los Alamos National Laboratory Report No. LAUR 86-748, 2000.
[21] L. B. Mendelsohn, F. Biggs, and J. B. Mann, Phys. Rev. A **2**, 1130 (1970).
[22] N. R. Werthamer, E. Helfand, and P. C. Hohenberg, Phys. Rev. **147**, 295 (1966).
[23] K. Maki, Phys. Rev. **148**, 362 (1966).
[24] W. L. McMillan, Phys. Rev. **167**, 331 (1968).
[25] V. K. Anand, A. D. Hillier, D. T. Adroja, A. M. Strydom, H. Michor, K. A. McEwen, and B. D. Rainford, Phys. Rev. B **83**, 064522 (2011).
[26] B. Mühlschlegel, Z. Phys. **155**, 313 (1959).
[27] J. Chen, L. Jiao, J. L. Zhang, Y. Chen, L. Yang, M. Nicklas, F. Steglich, and H. Q. Yuan, Phys. Rev. B **88**, 144510 (2013).
[28] P. E. Gregers-Hanse, M. Krusius, and G. R. Pickett, Phys. Rev. Lett. **27**, 38 (1971).
[29] H. M. Rosenberg, *Low Temperature Solid State Physics* (Oxford University Press, Oxford, 1963).